The structure of the Me_2-Dabco cation is very similar to those of the parent bicyclo[2.2.2]octanes and the quinuclidinium cation. The angles about the carbon and nitrogen atoms are all close to the tetrahedral value. The average of the C–C bond distances is 1.515(2) Å and of the C–N bond distances 1.503(6) Å. Table IV lists some structural parameters for the Me_2-Dabco cation and several closely related compounds. Both dynamic and static disorder in the form of a small twist of one-half of the molecule relative to the other half about the threefold axis is possible in these compounds.[46] The cation in this compound is completely ordered, however, with a twist angle of 5.5° (average of the three N–C–C–N dihedral angles). Spectroscopic measurements[47] require that the twist angle be 0 ± 4°, which is consistent with the data in Table III.

The thermal motions of the atoms are generally small. They may be qualitatively evaluated from Figures 1 and 2 which were drawn using Johnson's ORTEP program.[48] None of the vibration amplitudes exceeds 0.3 Å and most are less than 0.2 Å.

The packing of the ions is shown in Figure 4, and details of the hydrogen bonds are shown in Figure 5. Neighboring anions are linked together in layers parallel to the *yz* plane by hydrogen bonds with the intervening water molecules. The average H–N distance in the hydrogen bonds is about 2 Å, about normal for an O–H···N bond. The easy loss of crystal water to the atmosphere is therefore probably due to the channels running through the lattice, as can be seen in Figure 4, which allow diffusion of the water out of the crystal.

Acknowledgments. We wish to thank Dr. William P. Schaefer of the California Institute of Technology for his aid with the final refinement of the structure. The support of this research by the Research Corporation and by the Advanced Research Projects Agency is gratefully acknowledged.

(46) E. Deutsch, private communication; to be submitted for publication.
(47) A. H. Nethercott and A. Javan, *J. Chem. Phys.*, 21, 363 (1953).
(48) C. K. Johnson, "ORTEP: A Fortran Thermal Ellipsoid Plo Program for Crystal Structure Illustrations," Oak Ridge Nationa Laboratory, Oak Ridge, Tenn., Publication No. ORNL-3794, revised 1965.

Metal Complexes as Ligands. II.[1] The Synthesis, Structure Determination, and Bonding Characteristics of Certain Tin(IV) Halide Adducts of the Nickel(II) and Palladium(II) Dithiooxalato Complexes

Dimitri Coucouvanis,*[2] N. C. Baenziger, and S. M. Johnson

Contribution from the Department of Chemistry, University of Iowa, Iowa City, Iowa 52240. *Received November 21, 1972*

Abstract: The synthesis of anionic complexes of the general formula $[SnX_4O_2C_2S_2MS_2C_2O_2SnX_4]^{2-}$ (where M = Ni(II) or Pd(II); X = Cl, Br, I) is described. The structure of the benzyltriphenylphosphonium salt of the bis(dithiooxalato)nickel(II) bis(stannic chloride) complex, $[(C_7H_7)(C_6H_5)_3P]_2Ni(S_2C_2O_2)_2(SnCl_4)_2$, has been determined from three dimensional X-ray data collected by counter methods. The compound crystallizes in space group C_{2h}^5-$P2_1/a$ of the monoclinic system with two molecules in a cell defined by a = 14.487 (5), b = 26.334 (8), c = 9.912 (3) Å; β = 124.74 (4)°. The structure has been refined by least-squares methods to a final R factor on F of 2.5% based on 1831 observations above background. Anions containing only a single SnX_4 group have also been prepared and characterized (X = Cl, F). The structure of the $[(C_7H_7)(C_6H_5)_3P]_2Ni(S_2C_2O_2)_2SnCl_4$ complex has been determined. The compound crystallizes in space group C_{2h}^5-$P2_1/c$ with four molecules in a unit cell defined by a = 25.093 (15), b = 15.823 (9), c = 16.960 (8) Å; β = 119.55 (6)°. The structure has been refined to a final R factor on F of 6.72% based on 1724 observations above background. In both structures the Ni atoms are sulfur bonded, four coordinate, and planar and the Sn atoms are octahedrally coordinated. The structure of the planar bis(dithiooxalato)nickel(II) complex, $K_2Ni(S_2C_2O_2)_2$, previously reported by Cox, *et al.*, has been refined by a three-dimensional structural analysis of X-ray data collected by counter methods. Based on 1251 observations above background a final R factor on F of 4.84% was obtained. Infrared spectra are reported and assigned. The Ni–S stretching frequency, previously assigned on the basis of a normal coordinate analysis, was reassigned based on isotopic substitution experiments. Differences in the vibrational spectra and the structural parameters between the $[Ni(S_2C_2O_2)_2]^{2-}$ complex and its adducts suggest coordination of SnX_4 groups to the already coordinated dithiooxalate ligands results in a delocalization of charge away from the nickel atoms and a strengthening of the Ni–S bond by enhanced π back-bonding. Voltammetric studies of the adducts show reversible reduction waves. An explanation is offered for the redox properties and charge-transfer spectra of these compounds.

In recent communications[1,3,4] we have demonstrated that anionic dithiooxalate complexes can be used as ligands for coordinatively unsaturated metal complexes. In the resulting polynuclear molecules, the dithiooxalate complexes coordinate to the acceptor species either *via* the α-diketone portion of the co-

(1) Part I: D. Coucouvanis, *J. Amer. Chem. Soc.*, 92, 707 (1970).
(2) Alfred P. Sloan Fellow, 1972–1974.
(3) D. Coucouvanis, R. E. Coffman, and D. Piltingsrud, *J. Amer. Chem. Soc.*, 92, 5004 (1970).
(4) D. Coucouvanis, *J. Amer. Chem. Soc.*, 93, 1786 (1971).

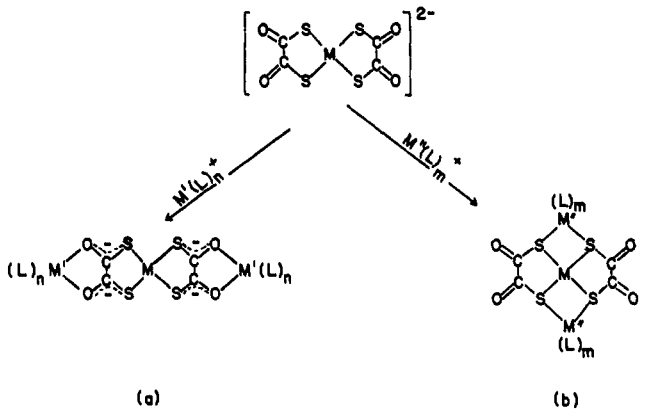

(a) (b)

Figure 1. Possible chelation modes of the $M(S_2C_2O_2)_2^{2-}$ complexes.

ordinated dithiooxalate ligand (Figure 1a) or *via* the already coordinated sulfur atoms[5] (Figure 1b). In this paper the synthesis, structures, and some properties of the stannic halide adducts of Ni(II) and Pd(II) dithiooxalate complex anions are reported.

Experimental Section

The chemicals in this research were used as purchased. Potassium dithiooxalate was obtained from S. H. Sargent Chemical Co. The anhydrous stannic halides were purchased from Rocky Mountain Research Inc. Analyses were performed by the analytical services laboratory of the Chemistry Department of The University of Iowa. Melting points recorded are uncorrected. Elemental ^{58}Ni and ^{62}Ni were purchased from Oak Ridge National Laboratory with an assayed purity of 99.89 and 98.83%, respectively.

Preparations of Complexes. (I) Bis(benzyltriphenylphosphonium)-bis(dithiooxalato)metal(II) Complexes. The $(Ph_3BzP)_2M(Dto)_2$ "parent" complexes were prepared from the potassium salts[6] by metathesis in water using Ph_3BzPCl. The precipitates that formed were dissolved in dimethylformamide (DMF), and ether was added until the first cloudiness appeared. The crystals which formed on cooling to 0° were isolated, washed with ether, and air-dried.

(A) $[(C_6H_5)_3P(C_7H_7)]_2[Ni(S_2C_2O_2)_2]$. Dark red crystals, yield 80%; mp 255–256°. *Anal.* Calcd: C, 64.50; H, 4.38. Found: C, 64.40; H, 4.43. X-Ray powder data:[7] 11.53 (s), 8.89 (w), 7.30 (m), 6.82 (vw), 6.28 (s), 5.86 (s), 5.29 (vw), 5.02 (m), 4.17 (m), 3.96 (s), 3.79 (m), 3.65 (m), 3.29 (s).

(B) $[(C_6H_5)_3P(C_7H_7)]_2[Pd(S_2C_2O_2)_2]$. Yellow crystals, yield 60%; mp 243–244°. *Anal.* Calcd: C, 61.65; H, 4.18. Found: C, 61.70; H, 4.21. X-Ray powder data:[7] 11.56 (s), 8.70 (w), 7.32 (m), 6.76 (vw), 6.20 (s), 5.80 (s), 5.28 (vw), 5.02 (m), 4.16 (m), 3.96 (s), 3.78 (m), 3.65 (m), 3.29 (s).

(II) Bis(benzyltriphenylphosphonium)bis(dithiooxalato)metal(II) Stannic Halide Adducts. Anhydrous conditions were used throughout. To a suspension containing 0.001 mol of $[(C_6H_5)_3P(C_7H_7)]_2[Ni(S_2C_2O_2)_2]$, prepared as described above, in 80 ml of CH_2Cl_2, 0.001 mol or 0.002 mol of stannic halide was added.[8] The resulting solution was filtered and diluted with about 200 ml of *n*-pentane. The crude solid or oil which formed was filtered off and recrystallized from appropriate solvent mixtures as indicated below specifically for each one of the complexes.

(C) $[(C_6H_5)_3P(C_7H_7)]_2[Ni(S_2C_2O_2)_2(SnCl_4)_2]$. Blue crystals, yield 66%; mp 219–220°. *Anal.* Calcd: C, 42.50; H, 2.88. Found: C, 42.37; H, 2.86. X-Ray powder data:[7] 8.87 (w), 7.99 (s), 7.05 (w), 6.57 (w), 5.43 (m), 4.78 (w), 4.16 (w), 3.91 (w), 3.51 (s). Recrystallization mixture 2:1 (v/v) CH_2Cl_2–ether.

(D) $[(C_6H_5)_3P(C_7H_7)]_2[Pd(S_2C_2O_2)_2(SnCl_4)_2]$. Orange crystals, yield 89%; mp 219–221°. *Anal.* Calcd: C, 41.24; H, 2.79. Found: C, 41.49, 41.10; H, 2.96, 2.86. X-Ray powder data:[7] 8.80 (w), 8.05 (s), 7.06 (w), 6.53 (w), 5.43 (m), 4.79 (w), 4.17 (w), 3.88 (w), 3.50 (s). Recrystallization mixture 1:1 (v/v) acetone–pentane.

(E) $[(C_6H_5)_3P(C_7H_7)]_2[Ni(S_2C_2O_2)_2(SnBr_4)_2]$. Blue crystals, yield 42%; mp 196–197°. *Anal.* Calcd: C, 34.45; H, 2.34. Found: C, 33.95; H, 2.36. X-Ray powder data:[7] 13.10 (w), 12.06 (w); 9.52 (m), 8.15 (s); 6.00 (m), 5.19 (m), 4.87 (m), 4.75 (m), 4.54 (m), 4.28 (w), 4.02 (m). Recrystallization mixture 2:3 (v:v) acetone–Skellysolve-B.

(F) $[(C_6H_5)_3P(C_7H_7)]_2[Pd(S_2C_2O_2)_2(SnBr_4)_2]$. Orange-red crystals, yield 85%; mp 209–210°. *Anal.* Calcd: C, 33.60; H, 2.28. Found: C, 32.99; H, 1.55. X-Ray powder data:[7] 12.95 (w), 12.00 (w), 9.52 (m), 8.23 (s), 5.97 (m), 5.28 (m), 4.86 (m), 4.73 (m), 4.52 (m), 4.27 (w), 4.01 (m). Recrystallization mixture 2:1 (v:v) CH_2Cl_2–pentane.

(G) $[(C_6H_5)_3P(C_7H_7)]_2[Ni(S_2C_2O_2)_2(SnI_4)_2]$. Green crystals, yield 88%; mp 135–136°. *Anal.* Calcd: C, 28.70; H, 1.95. Found: C, 28.35; H, 1.87. X-Ray powder data:[7] 10.96 (w), 9.56 (s), 8.95 (s), 7.09 (m), 5.87 (m), 5.62 (m), 4.65 (w), 4.00 (w), 3.33 (m). Recrystallization mixture 2:1 (v:v) CH_2Cl_2–pentane.

(H) $[(C_6H_5)_3P(C_7H_7)]_2[Pd(S_2C_2O_2)_2(SnI_4)_2]$. Red crystals, yield 90%; mp 152–153°. *Anal.* Calcd: C, 28.10; H, 1.91. Found: C, 27.13; H, 1.70. X-Ray powder data:[7] 10.94 (w), 9.54 (s), 8.93 (s), 7.11 (m), 5.88 (m), 5.61 (m), 4.66 (w), 4.02 (w), 3.31 (m). Recrystallization mixture 2:1 (v:v) CH_2Cl_2–pentane.

(I) $[(C_6H_5)_3P(C_7H_7)]_2[Ni(S_2C_2O_2)_2SnCl_4 \cdot H_2O]$. Blue crystals, yield 47%; mp 163–164°. *Anal.* Calcd: C, 50.48; H, 3.58. Found: C, 51.13; H, 3.28. X-Ray powder data:[7] 12.69 (w), 8.25 (m), 7.29 (s), 6.30 (m), 5.53 (m). Recrystallization mixture 2:1 (v:v) CH_2Cl_2–ether.

(J) $[(C_6H_5)_3P(C_7H_7)]_2[Pd(S_2C_2O_2)_2SnCl_4]$. Orange crystals, yield 68%; mp 168–169°. *Anal.* Calcd: C, 49.47; H, 3.35. Found: C, 49.35; H, 3.31. X-Ray powder data:[7] 12.62 (w), 8.08 (m), 7.18 (s), 6.19 (m), 5.42 (m). Recrystallization mixture 1:1 (v:v) acetone–pentane.

(K) $[(C_6H_5)_3P(C_7H_7)]_2[Ni(S_2C_2O_2)_2SnF_4]$. For the preparation of this complex the procedure was modified slightly in that the reaction solvent was 100 ml of a 1:1 (v:v) mixture of dichloromethane–acetone. The system was boiled for 5 min. The intensely blue solution was filtered and diluted with 150 ml of anhydrous ether. The resulting floculent precipitate was recrystallized from a 2:1 (v/v) CH_2Cl_2–pentane. Blue crystals, yield 58%; mp 185–186°. *Anal.* Calcd: C, 54.02; H, 3.45. Found: C, 53.85; H, 3.45.

All of the complexes were found to be diamagnetic and 2:1 electrolytes[9] in nitromethane. In donor solvents they readily dissociate to the parent $M(Dto)_2^{2-}$ complex and the corresponding stannic halide.

Physical Measurements. Magnetic susceptibilities were determined at ambient room temperature using a Faraday technique. The calibrant was $Hg(Co(SCN)_4)$.[12] Near-infrared spectra were obtained with a Perkin-Elmer 421 recording spectrophotometer, frequency calibrated with polystyrene. Far-infrared spectra spanning the frequency range 600–100 cm^{-1} were obtained on a Beckman I.R. 11 spectrometer equipped with a triglycine sulfate crystal detector and frequency calibrated with water vibrations occurring within that wavelength range. Ultraviolet, visible, and near-infrared spectra were obtained with a Cary Model 14 recording spectrophotometer using 1-cm quartz cells. A Debye–Scherrer camera utilizing nickel-filtered copper radiation was used to observe the X-ray powder patterns of the complexes. Nonius Weissenberg and Precession cameras were used for the single-crystal preliminary alignments and space group determinations. Intensity data were collected on a Picker FACS I automated four-circle diffractometer equipped with a graphite single-crystal monochromator and pulse height analyzer.

Conductivity studies in distilled acetonitrile or spectral grade nitromethane were performed using a Beckman Model RC 16B2 conductivity bridge and a Yellow Springs Instrument Co., Inc., 3502 conductivity cell.

(5) (a) D. Coucouvanis, Papers presented at the 157th National Meeting of the American Chemical Society, Minneapolis, Minn., April 1969; (b) the 162nd National Meeting, Washington, D. C., September 1971; (c) D. Coucouvanis and D. Piltingsrud, *J. Amer. Chem. Soc.*, in press.

(6) C. S. Robinson and H. O. Jones, *J. Chem. Soc.*, 62 (1912).

(7) *d* spacings, Å, of some strong lines.

(8) Aliquots of a 0.5 *M* CH_2Cl_2 solution of anhydrous $SnCl_4$ were used in the preparation of the stannic halide adducts.

(9) The equivalent conductances, Λ, of 1×10^{-3} *M* solutions of these complexes in nitromethane are similar to values reported[10] in the literature for 2:1 electrolytes (*ca.* 160–180 ohm^{-1} cm^{-1}). However, conductance studies as a function of concentration for these complexes indicate incomplete ionic dissociation as evidenced by the nonlinearity of $\sqrt{c}$ *vs.* Λ plots.[11]

(10) J. P. Fackler, Jr., and D. Coucouvanis, *J. Amer. Chem. Soc.*, 88, 3913 (1966).

(11) R. D. Feltham and R. G. Hayter, *J. Chem. Soc.*, 4587 (1964).

(12) B. N. Figgis and R. S. Nyholm, *J. Chem. Soc.*, 4190 (1958).

Table I. Crystal Intensity Measurement and Structure Determination Data

Compound	$K_2NiS_4C_4O_4$	$Sn_2NiCl_8S_4P_2O_4C_{54}H_{44}$	$SnNiCl_4S_4P_2O_4C_{54}H_{44}\cdot H_2O$
Mol wt, amu	377.3	1526.3	1283.6
Cell dimensions, Å	$a = 22.516 \pm 0.011$	$a = 14.487 \pm 0.005$	$a = 25.093 \pm 0.015$
	$b = 7.863 \pm 0.004$	$b = 26.334 \pm 0.008$	$b = 15.823 \pm 0.009$
	$c = 11.088 \pm 0.006$	$c = 9.912 \pm 0.003$	$c = 16.960 \pm 0.008$
	$\beta = 143.92 \pm 0.02°$	$\beta = 124.74 \pm 0.04°$	$\beta = 119.55 \pm 0.06°$
Density, g cm^{-3}			
obsd	2.23 ± 0.05[a]	1.50 ± 0.05[b]	1.49 ± 0.05[a]
calcd	2.20	1.48	1.45
Z	4	2	4
Space group	C_2/c[c]	$P2_1/a$[d]	$P2_1/c$[e]
λ	Mo Kα (0.7107 Å)[f]	Mo Kα (0.7107 Å)[g]	Mo Kα (0.7107 Å)[f]
μ, cm^{-1}	31.0	16.6	12.8
Crystal dimensions, mm	$0.31 \times 0.17 \times 0.47$	$0.22 \times 0.18 \times 0.26$	$0.26 \times 0.37 \times 0.10$
Reflections measured	4222	7091	6129
Takeoff angle	3.0°	3.0°	4.0°
2θ range	$0° < 2\theta < 70°$	$0° < 2\theta < 50°$	$0° < 2\theta < 85°$
Scan width[h]	1.30°	1.10°	1.20°
Unique reflections	1661	2459	2378
Atoms in asymmetric unit	8	38 (+22 H)	71 (+46 H)
Final R_1	0.048	0.025	0.067
Final R_2	0.052	0.029	0.075
Reflections used in refinement	1212	1831	1724
Number of parameters	69	420	635
SDOUW[i]	2.17	1.05	2.25

[a] Determined by flotation in a CCl_4–CI_4 mixture. [b] Determined by flotation in a CS_2–CBr_4 mixture. [c] Systematic absences: hkl for $h + k \neq 2n$ and $h0l$ for $h, l \neq 2n$. [d] Systematic absences: $h0l$ for $h \neq 2n$ and $0k0$ $k \neq 2n$. [e] Systematic absences: $h0l$ for $l \neq 2n$ and $0k0$ $k \neq 2n$. [f] A graphite single-crystal monochromator was used. [g] Zirconium filters were used. [h] A 2θ scan data collection procedure was used. [i] Standard deviation of a reflection of unit weight.

Cyclic voltammetry data were obtained on a Chemtrix Model SSP-2 polarograph equipped with a Tektronix storage oscilloscope. The working electrode was a 1.0 mm diameter platinum sphere. The half-wave potentials reported have an estimated precision of 0.01 V. The potentials at which $Ni(MNT)_2^{2-}$ undergoes oxidation were determined to be +0.18 and +1.25 V. The electrochemistry of the complexes was studied in doubly distilled methylene chloride with tetra-*n*-butylammonium perchlorate as supporting electrolyte. Stability of the starting potentials was achieved only at an electrolyte concentration of 0.2 *M*. The preparation of the Ag/AgI reference electrode has been described in the literature.[13] A modified version of the cell employed by Röhrscheid, *et al.*,[13] was used for the electrochemical measurements.

The potentials[14] reported are internally calibrated relative to the potential at which $Ni(MNT)_2^-$ undergoes reduction (−0.18 V). The use of $(Bu_4N)Ni(MNT)_2$ as an internal standard does not alter the results since addition of a small amount of this compound to solutions of the adducts did not affect the position of the voltammetric waves. Similarly the reduction potential of the internal standard was not affected by the presence of the stannic halide adducts.

X-Ray Diffraction Measurements. Collection and Reduction of Data. Specific details concerning crystal characteristics and X-ray diffraction methodology are shown in Table I. For each one of the structures, a set of unit cell parameters was derived from the observed diffractometer settings x, ϕ, and 2θ for three independent reflections. These were refined by a least-squares technique to give the best fit between calculated and observed setting x, ϕ, and 2θ for 12 independent reflections carefully centered on the diffractometer. The results are shown in Table I.

Intensity data for all structures were obtained by the moving crystal–moving counter technique on an automated diffractometer. A scan speed of 1°/min in 2θ was used and the background for each reflection was determined by 10-sec counts at either end of the scan range. At regular intervals (*i.e.*, 40–100 reflections) three "standard" reflections were measured in order to monitor the data collection. No change in crystal quality or instrument performance was detected in any of the structural determinations.

The observed intensities were corrected for background, Lorentz, and polarization effects.[15] Scattering factors for the zerovalent atoms were obtained from the International Tables.[16] Where appropriate the calculated structure factors were corrected for the effects of anomalous dispersion[17] of the tin, nickel, potassium, sulfur, chlorine, and phosphorus atoms.[18]

The standard deviation in the integrated intensities was computed in two ways: (a) from counting statistics

$$\sigma_{(I)} = \left(\frac{\sum I + \sum B}{n}\right)^{1/2}$$

where I is the total count in the 2θ scan, B is the total background count adjusted for scan time, and n is the number of equivalent reflections, and (b) from agreement between equivalent reflections if two or more such measurements were made

$$\sigma_{(I)} = \left[\frac{\sum (I_d - I_{d(av)})^2}{n - 1}\right]^{1/2}$$

where $I_d = I - B$. The largest estimate of the standard deviation was chosen. Experimental weights were used and defined as $w = 1/\sigma^2(F)$. A unique reflection was excluded from the least-squares refinement calculations whenever $I_d < 3\sigma(B)$ (where I_d and B are defined above). In all cases the function minimized was $\Sigma w(|F_o| - |F_c|)^2$ and the progress of the refinement was judged by the values of the residuals R_1 and R_2.[19]

(13) F. Röhrscheid, A. L. Balch, and R. H. Holm, *Inorg. Chem.*, 5, 1542 (1966).

(14) The values of the potentials previously reported[1] are incorrect due to an undetected malfunction of the potentiometer. $Ni(MNT)_2^{2-}$ is an abbreviation for the $[NiS_4C_4(CN)_4]^{2-}$ complex.

(15) Lorentz andp olarization corrections, electron density calculations, and full-matrix as well as block diagonal least-squares calculations were carried out on an IBM 360-65 computer using programs written by Professor N. C. Baenziger of the University of Iowa. Computer drawings were obtained using Johnson's ORTEP thermal ellipsoid plotting program. In the block diagonal least-squares calculations 4×4 and 9×9 blocks were used for isotropic and anisotropic refinement, respectively.

(16) "International Tables for X-Ray Crystallography," Vol. III, 2nd ed, Kynoch Press, Birmingham, England, 1965, pp 202, 204.

(17) See ref 16, p 213.

(18) No absorption correction has been applied to any of the three data sets. The values of the linear absorption coefficients are shown in Table I.

(19) $R_1 = \Sigma|\Delta F|/\Sigma|F_o|$, $R_2 = [\Sigma w(\Delta F)^2/\Sigma w|F_o|^2]^{1/2}$.

Table II. Final Positional and Thermal Parameters for the Atoms in $K_2Ni(Dto)_2$[a]

Atom	$x \times 10^4$	$y \times 10^4$	$z \times 10^4$	10^3U_{11}[b]	10^3U_{22}	10^3U_{33}	10^3U_{12}	10^3U_{13}	10^3U_{23}
Ni	0 (0)	1173 (2)	2500 (0)	50 (1)	42 (2)	57 (1)	0 (0)	46 (1)	0 (0)
K	3026 (1)	1233 (3)	2817 (3)	81 (2)	54 (2)	104 (2)	−5 (1)	81 (2)	−7 (1)
S(1)	597 (2)	3187 (3)	2336 (4)	76 (2)	44 (2)	94 (3)	1 (1)	76 (2)	2 (1)
S(2)	751 (2)	−821 (3)	2700 (3)	75 (2)	38 (2)	87 (2)	3 (1)	71 (2)	4 (1)
C(1)	1440 (6)	218 (11)	2697 (13)	66 (9)	52 (10)	68 (9)	−10 (5)	54 (8)	−5 (5)
C(2)	1343 (6)	2174 (10)	2483 (12)	54 (8)	48 (8)	60 (9)	5 (5)	43 (8)	0 (5)
O(1)	1978 (5)	−493 (8)	2877 (10)	109 (8)	62 (8)	172 (10)	10 (4)	131 (9)	2 (5)
O(2)	1807 (4)	2915 (8)	2457 (10)	86 (7)	70 (8)	132 (9)	2 (4)	99 (8)	7 (4)

[a] In this and the following tables, standard deviations of the least significant figure(s) are given in parentheses. [b] The U values given in this table are defined by the temperature factor expression $\exp[-\pi^2(h^2a^{*2}U_{11} + k^2b^{*2}U_{22} + l^2c^{*2}U_{33} + 2hka^*b^*U_{12} + 2hla^*c^*U_{13} + 2klb^*c^*U_{23})]$.

Determination of the Structures. (a) $Ni(Dto)_2K_2$. The approximate atomic coordinates previously reported by Cox, *et al.*,[20] and isotropic temperature factors for all atoms were refined by full-matrix least squares and converged to values of 0.0945 and 0.0940, respectively, for R_1 and R_2.[19] At this stage each atom was assigned an anisotropic temperature factor of the form $\exp(-\beta_{11}h^2 - \beta_{22}k^2 - \beta_{33}l^2 - 2\beta_{12}hk - 2\beta_{13}hl - 2\beta_{23}kl)$ and continued refinement resulted in the final values of 0.048 and 0.052 for R_1 and R_2, respectively. A final difference map showed no additional peaks.

(b) $Ni(Dto)_2(SnCl_4)_2(BzPh_3P)_2$. From the intensity data, corrected for background, Lorentz, and polarization effects,[15,18] a set of structure factors was obtained which was used to compute a three-dimensional Patterson map. Solution of the Patterson yielded the location of the tin, the nickel (at the center of symmetry), and two chlorine atoms. The remaining atoms were located following successive structure factor, Fourier syntheses, and least-squares refinement calculations. Isotropic temperature factors and the positional parameters of all 38 atoms in the asymmetric unit were refined by a block diagonal least-squares method[15] to values of 0.058 and 0.061 for R_1 and R_2, respectively. At this point anisotropic temperature factors were assigned to all the atoms of the complex anion. Subsequent refinement resulted in values for R_1 and R_2 of 0.047 and 0.052, respectively. Anisotropic temperature factors were assigned to the remaining nonhydrogen atoms and after three cycles of refinement R_1 and R_2 converged to 0.038 and 0.043, respectively. A difference Fourier map now showed several peaks of 1.0 e/Å^3 (where the average value for a carbon atom is 6–8 e/Å^3); all of the 22 hydrogen atoms were located and assigned temperature factors equal to the isotropic temperature factors of the carbon atoms adjacent to them. Block diagonal refinement of the positional and thermal parameters of the hydrogen atoms resulted in residuals R_1 and R_2 of 0.0250 and 0.0299, respectively.

(c) $Ni(Dto)_2(SnCl_4)(BzPh_3P)_2 \cdot H_2O$. The intensity data treated as previously described were used to compute a Patterson map which revealed the positions of the tin, nickel, and one of the chlorine atoms. Subsequent structure factor, Fourier syntheses, difference Fourier syntheses, and least-squares refinement calculations revealed all the nonhydrogen atoms. Isotropic temperature factors and the positional parameters of all 71 nonhydrogen atoms in the asymmetric unit were refined by a block diagonal least-squares method[15] to values of 0.109 and 0.115 for R_1 and R_2, respectively. At this point anisotropic temperature factors were assigned to all the atoms in the complex anion. Refinement resulted in values for R_1 R_2 of 0.087 and 0.092, respectively. Anisotropic temperature factors were then assigned to the rest of the nonhydrogen atoms and all parameters were refined to values for R_1 and R_2 of 0.067 and 0.075, respectively. No attempt was made to locate the hydrogen atoms.

Crystallographic Results[21]

Atomic positional parameters with standard deviations derived from the inverse matrix of the last least squares refinement are compiled in Tables II, IV, and VI for the structures of $K_2Ni(Dto)_2$, $(BzPh_3P)_2Ni(Dto)_2$-$(SnCl_4)_2$, and $(BzPh_3P)_2Ni(Dto)_2SnCl_4$, respectively. Intramolecular bond distances and angles are given in Tables III, V, and VII. The atom labeling schemes are shown in Figures 2, 3, and 4.

Table III. Intramolecular Bond Distances (Å) and Angles (deg) for $K_2Ni(Dto)_2$

Ni–K	6.533 (3)	K–O(2)	2.770 (6)
Ni–S(1)	2.178 (3)	S(1)–S(1)	2.990 (4)
Ni–S(2)	2.181 (3)	S(1)–S(2)	3.160 (3)
Ni–C(1)	3.158 (9)	S(1)–C(1)	2.825 (9)
Ni–C(2)	3.140 (9)	S(1)–C(2)	1.744 (9)
Ni–O(1)	4.329 (11)	S(2)–S(2)	3.033 (4)
Ni–O(2)	4.329 (9)	S(2)–C(1)	1.756 (9)
K–S(1)	5.277 (4)	S(2)–C(2)	2.811 (9)
K–S(2)	5.272 (4)	C(1)–C(2)	1.544 (10)
K–C(1)	3.556 (9)	C(1)–O(1)	1.197 (10)
K–C(2)	3.574 (9)	C(2)–O(2)	1.216 (10)
K–O(1)	2.768 (6)	O(1)–O(2)	2.694 (8)
S(1)–Ni–S(2)	92.9 (1)	C(2)–C(1)–S(2)	116.7 (8)
O(1)–K–O(2)	74.2 (2)	C(1)–C(2)–O(2)	117.6 (10)
Ni–S(1)–C(2)	105.8 (3)	C(1)–C(2)–S(1)	118.3 (9)
Ni–S(2)–C(1)	106.2 (3)	K–O(2)–C(2)	122.5 (6)
C(2)–C(1)–O(1)	119.3 (10)	K–O(1)–C(1)	122.4 (7)

Results and Discussion

Synthesis and General Characteristics. The stoichiometries of the adducts formed were a function of the stannic halide and the solvent used in the syntheses. With SnF_4 only a 1:1 adduct could be formed regardless of the amount of excess SnF_4 used. With $SnCl_4$ both the 2:1 and 1:1 adducts could be prepared when the solvent was dichloromethane or acetone; in acetonitrile, however, only the 1:1 $SnCl_4$ adducts formed. This was also verified by a continuous variation study in CH_3CN, between *n*-$BuSnCl_3$ and both the $Ni(Dto)_2^{2-}$ and $Pd(Dto)_2^{2-}$ complexes. Solvent effects of this nature are not surprising since both acetonitrile[22,23] and acetone[24] are known to form adducts with anhydrous stannic halides. It is presumed that the degree of solvent–stannic halide interaction is crucial in the synthesis of the dithiooxalate–stannic halide adducts.

In strong donor solvents (*i.e.*, dimethyl sulfoxide, dimethylformamide, etc.) solvolysis proceeds very rapidly $(C_2M(Dto)_2(SnX_4)_2 + 4L \rightarrow C_2M(Dto)_2 + 2SnX_4L_2)$ as evidenced by the appearance of the

(20) E. G. Cox, W. Wardlaw, and K. C. Webster, *J. Chem. Soc.*, 1475 (1935).

(21) A compilation of observed and calculated structure factor amplitudes and the relative weights of individual reflections as well as atomic thermal parameters will appear following these pages in the microfilm edition of this volume of the journal. Single copies may be obtained from the Business Operations Office, Books and Journals Division, American Chemical Society, 1155 Sixteenth St., N.W., Washington, D. C. 20036 by referring to code number JACS-73-3875. Remit check or money order for $5.00 for photocopy or $2.00 for microfiche.

(22) T. L. Brown and M. Kubota, *J. Amer. Chem. Soc.*, 83, 5175 (1961).

(23) M. F. Farona and J. Grasselli, *Inorg. Chem.*, 6, 1675 (1967).

(24) I. Lindquist, "Inorganic Adduct Molecules of Oxo-Compounds," Academic Press, New York, N. Y., 1963, p 12.

Table IV. Final Positional[a] Parameters for the Atoms in $(BzPh_3P)_2Ni(Dto)_2(SnCl_4)_2$

Atom	x	y	z	Atom	x	y	z
		×10⁵				×10³	
Sn	21539 (4)	16169 (3)	−3645 (6)	H(4)	−144 (5)	310 (3)	−384 (7)
				H(5)	0 (5)	307 (3)	−94 (7)
				H(6)	71 (5)	381 (3)	−463 (8)
		×10⁴		H(7)	170 (6)	348 (3)	−1 (8)
Ni	5000 (0)	0 (0)	0 (0)	H(8)	−87 (5)	345 (3)	−537 (8)
Cl(1)	3460 (2)	2291 (1)	412 (3)	H(10)	561 (7)	363 (4)	433 (10)
Cl(2)	675 (2)	2001 (1)	−2775 (2)	H(11)	432 (6)	529 (3)	−269 (9)
Cl(3)	1739 (2)	1820 (1)	1546 (2)	H(12)	104 (5)	468 (3)	−325 (7)
Cl(4)	1226 (2)	805 (1)	−989 (3)	H(13)	269 (5)	578 (3)	−401 (7)
S(1)	5031 (2)	443 (1)	1885 (3)	H(14)	451 (5)	446 (3)	−127 (7)
S(2)	3844 (2)	528 (1)	−1942 (3)	H(15)	255 (7)	467 (3)	88 (9)
P	2761 (2)	3909 (1)	−1290 (2)	H(17)	349 (8)	480 (4)	352 (11)
O(1)	3667 (4)	1170 (2)	1438 (5)	H(18)	480 (7)	336 (3)	172 (10)
O(2)	2787 (4)	1283 (2)	−1730 (6)	H(19)	498 (7)	437 (4)	530 (10)
C(1)	4021 (6)	873 (4)	819 (8)	H(20)	97 (6)	548 (3)	−417 (8)
C(2)	3481 (6)	926 (4)	−1005 (8)	H(21)	119 (6)	299 (3)	−776 (9)
C(3)	1375 (6)	3662 (3)	−2108 (8)	H(22)	112 (5)	241 (3)	−597 (8)
C(4)	−693 (6)	3202 (4)	−3373 (10)	H(23)	336 (7)	388 (4)	−429 (10)
C(5)	119 (6)	3213 (4)	−1693 (9)	H(24)	235 (8)	375 (4)	−698 (11)
C(6)	566 (6)	3653 (3)	−3807 (8)	H(26a)	371 (6)	316 (3)	905 (9)
C(7)	1164 (6)	3444 (4)	−1027 (8)	H(26b)	436 (6)	356 (3)	863 (9)
C(8)	−445 (6)	3428 (4)	−4389 (8)	H(27)	221 (6)	276 (3)	−335 (8)
C(9)	2684 (6)	4519 (3)	−2218 (8)				
C(10)	4976 (7)	3799 (4)	3741 (9)				
C(11)	3627 (7)	5171 (4)	−2666 (10)				
C(12)	1685 (6)	4807 (3)	−3054 (9)				
C(13)	2642 (7)	5464 (4)	−3500 (8)				
C(14)	3663 (6)	4701 (4)	−2018 (9)				
C(15)	3230 (6)	4435 (3)	1450 (8)				
C(16)	3531 (6)	4015 (3)	927 (8)				
C(17)	3819 (7)	4542 (4)	3170 (9)				
C(18)	4396 (6)	3680 (4)	2031 (9)				
C(19)	4670 (7)	4206 (4)	4231 (9)				
C(20)	1672 (7)	5274 (4)	−3695 (9)				
C(21)	1623 (7)	3064 (4)	−6768 (9)				
C(22)	1548 (7)	2757 (4)	−5697 (10)				
C(23)	2934 (7)	3610 (4)	−4594 (9)				
C(24)	2295 (8)	3480 (4)	−6247 (10)				
C(25)	2882 (6)	3307 (3)	−3472 (8)				
C(26)	3553 (6)	3453 (3)	−1661 (7)				
C(27)	2200 (7)	2893 (4)	−3997 (9)				

[a] A table containing the anisotropic thermal parameters has been deposited and will appear in the microfilm version of this journal (ref 21).

characteristic bright color of the $C_2M(Dto)_2$ complexes (where C is a cation). Acetone solutions of $C_2M(Dto)_2$-$SnCl_4$ disproportionate on standing according to the reaction $2C_2M(Dto)_2SnCl_4 \rightarrow C_2M(Dto)_2 + C_2M(Dto)_2$-$(SnCl_4)_2$. On standing in air the blue crystals of the 1:1 stannic fluoride adduct readily hydrolyze as indicated by the appearance of the characteristic red color of the "parent" $Ni(Dto)_2^{2-}$ complex.

The complexes of Ni(II) and Pd(II) with identical empirical formulas are X-ray isomorphous. However, 2:1 adducts of the same dithiooxalate metal complex with different stannic halides are not isomorphous.

Infrared Spectra. The infrared spectrum of the potassium "salt" of the $Pt(Dto)_2^{2-}$ complex anion has been interpreted on the basis of a normal coordinate analysis.[25] Very similar spectra are obtained for the X-ray isomorphous[20] Pd(II) and Ni(II) complexes. The infrared spectra of the dithiooxalates and their stannic halide adducts differ primarily in the position of two bands. In the "parent" complexes, a broad band near 1600 cm^{-1} has been assigned to the C–O stretching vibrations while a band at 1083 cm^{-1} is attributed to a combination of the C–C and C–S stretching vibrations.[25] In the spectra of the stannic halide adducts the C–O stretching vibrations occur between 1480 and 1450 cm^{-1} while the C–C + C–S combination band is found between 1140 and 1150 cm^{-1}.

The bathochromic shift of the C–O stretching frequency and the hypsochromic shift of the C–C + C–S combination band reflect the delocalization of charge toward the stannic halide moiety which results in a reduction of the C–O bond order and an increase in the C–S bond order.

Whereas only one broad absorption, corresponding to the perturbed C–O vibration, is observed in the spectra of the 2:1 adducts at 1480 cm^{-1}, two such absorptions are found in the spectra of the 1:1 adducts, at 1640–1612 and 1445–1448 cm^{-1}, and are due to the presence of both perturbed and unperturbed dithiooxalate ligands, Table VIII. The position of the low-energy C=O stretch at 1445 cm^{-1} in the 1:1 adducts suggests that in these compounds the perturbation on the bridging ligand is even greater than that observed in the 2:1 adducts. Also the position of the high-energy C–O stretching vibration (1640 cm^{-1}) in the

(25) J. Fujita and K. Nakamoto, *Bull. Chem. Soc. Jap.*, 37, 528 (1964).

Table V. Intramolecular Bond Distances and Angles for $(BzPh_3P)_2Ni(Dto)_2(SnCl_4)_2$

Bond lengths, Å		Bond angles, deg			
		A. Anion			
Sn–Cl(1)	2.380 (3)	Cl(1)–Sn–Cl(2)	96.0 (1)	Cl(3)–Sn–O(2)	166.3 (2)
Sn–Cl(2)	2.342 (2)	Cl(1)–Sn–Cl(3)	95.3 (1)	Cl(4)–Sn–O(1)	83.5 (2)
Sn–Cl(3)	2.352 (2)	Cl(1)–Sn–Cl(4)	165.6 (1)	Cl(4)–Sn–O(2)	81.6 (2)
Sn–Cl(4)	2.411 (3)	Cl(1)–Sn–O(1)	84.0 (2)	O(1)–Sn–O(2)	73.5 (2)
Sn–O(1)	2.218 (5)	Cl(1)–Sn–O(2)	87.9 (2)	S(1)–Ni–S(2)	92.6 (1)
Sn–O(2)	2.205 (5)	Cl(2)–Sn–Cl(3)	102.6 (1)	C(1)–S(1)–Ni	103.7 (3)
Ni–S(1)	2.182 (2)	Cl(2)–Sn–Cl(4)	93.9 (1)	C(2)–S(2)–Ni	103.7 (3)
Ni–S(2)	2.183 (2)	Cl(2)–Sn–O(1)	163.8 (1)	Sn–O(1)–C(1)	115.1 (5)
S(1)–S(2)	3.156 (3)	Cl(2)–Sn–O(2)	90.3 (1)	Sn–O(2)–C(2)	115.2 (5)
$S(1)_r$–S(2)	3.015 (4)	Cl(3)–Sn–Cl(4)	92.7 (1)	O(1)–C(1)–S(1)	124.3 (5)
S(1)–C(1)	1.667 (8)	Cl(3)–Sn–O(1)	93.5 (1)	O(2)–C(2)–S(2)	123.6 (5)
S(2)–C(2)	1.673 (8)				
O(1)–O(2)	2.647 (6)				
O(1)–C(1)	1.268 (9)				
O(2)–C(2)	1.259 (10)				
C(1)–C(2)	1.513 (10)				
		B. Cation			
Av phenyl ring C–C dist		1.40 (2)[a,b]	Av phenyl ring C–C–C angle		119.8 (2)
Av P–phenyl C dist		1.82 (2)	Av C–P–C angle		109.5 (2)
P–benzyl C		1.84 (1)	Av external C–phenyl angle		119.6 (2)
Benzyl C–C		1.53 (1)	Benzyl C–C angle		110.4 (6)
Av phenyl ring C–H dist		0.97 (10)	Av phenyl ring–H angle		120 (1)
Av benzyl C–H dist		1.03 (8)	Av benzyl C–H angle		108 (1)

[a] In this and following tables, the quantity in parentheses following an average value is given by the expression $s = \sqrt{\Sigma \Delta d^2/(n-1)}$ where Δd is the difference between an individual quantity and the mean value for that quantity. [b] Detailed information on the individual C–C distances in the cation has been deposited (see ref 21).

Table VI. Final Positional[a] Parameters for the Atoms in $(BzPh_3P)_2Ni(Dto)_2SnCl_4 \cdot H_2O$

Atom	x	y	z	Atom	x	y	z
		×10⁴				×10³	
Sn	1686 (10)	286 (10)	−2958 (10)	C(17)	344 (10)	626 (17)	−566 (13)
				C(18)	378 (10)	570 (14)	−593 (14)
				C(19)	552 (8)	673 (13)	−254 (12)
		×10³		C(20)	638 (11)	535 (16)	−191 (16)
Ni	319 (1)	321 (2)	−112 (2)	C(21)	527 (12)	590 (16)	−279 (16)
Cl(1)	169 (4)	10 (6)	−157 (6)	C(22)	574 (11)	522 (14)	−243 (15)
Cl(2)	181 (4)	66 (5)	−422 (5)	C(23)	618 (9)	688 (14)	−198 (13)
Cl(3)	199 (3)	−112 (5)	−295 (5)	C(24)	656 (11)	613 (15)	−169 (17)
Cl(4)	62 (3)	19 (5)	−384 (6)	C(25)	617 (10)	997 (15)	−136 (14)
S(1)	412 (3)	338 (4)	−11 (4)	C(26)	545 (9)	856 (14)	−236 (13)
S(2)	223 (4)	301 (5)	−211 (7)	C(27)	557 (9)	867 (16)	−148 (14)
S(3)	299 (3)	453 (5)	−108 (6)	C(28)	595 (10)	936 (16)	−96 (14)
S(4)	339 (3)	189 (4)	−120 (4)	C(29)	568 (9)	910 (13)	−278 (14)
P(1)	75 (3)	723 (5)	−544 (5)	C(30)	606 (11)	980 (14)	−227 (16)
P(2)	503 (3)	766 (4)	−296 (4)	C(31)	−73 (13)	618 (21)	−824 (18)
O(1)	263 (6)	64 (9)	−212 (10)	C(32)	−84 (10)	691 (19)	−792 (15)
O(2)	163 (7)	163 (10)	−275 (13)	C(33)	13 (10)	670 (15)	−655 (13)
O(3)	370 (7)	576 (10)	−14 (12)	C(34)	−18 (14)	571 (19)	−773 (17)
O(4)	471 (17)	477 (12)	72 (12)	C(35)	29 (13)	596 (15)	−683 (17)
C(1)	426 (9)	445 (14)	24 (13)	C(36)	−41 (10)	724 (17)	−709 (15)
C(2)	213 (11)	192 (17)	−233 (17)	C(37)	127 (9)	779 (14)	−570 (14)
C(3)	268 (10)	138 (15)	−193 (15)	C(38)	138 (12)	870 (17)	−547 (15)
C(4)	367 (8)	504 (14)	−29 (13)	C(39)	188 (16)	905 (19)	−560 (20)
C(5)	48 (12)	804 (16)	−490 (18)	C(40)	155 (11)	727 (18)	−610 (18)
C(6)	475 (10)	788 (14)	−419 (14)	C(41)	198 (12)	771 (17)	−626 (19)
C(7)	439 (9)	752 (13)	273 (13)	C(42)	212 (11)	857 (16)	−600 (15)
C(8)	345 (11)	740 (14)	−235 (15)	C(43)	115 (11)	641 (14)	−466 (15)
C(9)	388 (9)	807 (14)	−324 (13)	C(44)	79 (12)	576 (15)	−463 (16)
C(10)	340 (11)	802 (14)	−306 (15)	C(45)	205 (14)	597 (19)	−347 (20)
C(11)	396 (10)	683 (16)	−183 (17)	C(46)	101 (11)	516 (16)	−395 (16)
C(12)	443 (10)	693 (14)	−204 (12)	C(47)	181 (15)	657 (17)	−407 (16)
C(13)	442 (10)	708 (15)	−475 (14)	C(48)	166 (13)	525 (17)	−332 (15)
C(14)	374 (9)	700 (17)	−506 (13)	C(49)	−53 (11)	736 (21)	−511 (18)
C(15)	477 (10)	651 (14)	−495 (14)	C(50)	4 (11)	748 (16)	−461 (13)
C(16)	445 (10)	583 (15)	−556 (13)	C(51)	−77 (13)	677 (19)	−469 (18)
O_{H_2O}	237 (8)	272 (13)	505 (12)	C(52)	−44 (12)	643 (21)	−381 (17)
				C(53)	14 (12)	668 (18)	−334 (15)
				C(54)	45 (13)	720 (18)	−371 (19)

[a] A table containing the anisotropic thermal parameters has been deposited and will appear in the microfilm version of this journal (ref 21).

Table VII. Intramolecular Bond Distances and Angles[a] for $(BzPh_3P)_2Ni(Dto)_2SnCl_4$ Anion

Bond lengths, Å				Bond angles, deg			
Sn–Cl(1)	2.380 (8)	S(2)–S(4)	3.09 (1)	Cl(1)–Sn–Cl(2)	170.0 (3)	O(1)–Sn–O(2)	76.9 (6)
Sn–Cl(2)	2.379 (8)	S(2)–C(2)	1.77 (3)	Cl(1)–Sn–Cl(3)	91.5 (3)	S(1)–Ni–S(3)	91.7 (3)
Sn–Cl(3)	2.346 (7)	S(3)–C(4)	1.76 (2)	Cl(1)–Sn–Cl(4)	94.0 (3)	S(1)–Ni–S(4)	88.6 (3)
Sn–Cl(4)	2.329 (7)	S(4)–C(3)	1.78 (2)	Cl(1)–Sn–O(1)	85.0 (5)	S(2)–Ni–S(3)	88.7 (3)
Sn–O(1)	2.154 (13)	O(1)–O(2)	2.69 (2)	Cl(1)–Sn–O(2)	86.1 (6)	S(2)–Ni–S(4)	91.2 (3)
Sn–O(2)	2.168 (16)	O(1)–C(3)	1.20 (3)	Cl(2)–Sn–Cl(3)	93.3 (3)	C(1)–S(1)–Ni	110.4 (7)
Ni–S(1)	2.136 (7)	O(2)–C(2)	1.19 (3)	Cl(2)–Sn–Cl(4)	93.2 (3)	C(2)–S(2)–Ni	106.6 (9)
Ni–S(2)	2.171 (8)	O(3)–O(4)	2.71 (3)	Cl(2)–Sn–O(1)	86.6 (4)	C(4)–S(3)–Ni	108.7 (8)
Ni–S(3)	2.156 (9)	O(3)–C(4)	1.17 (3)	Cl(2)–Sn–O(2)	86.9 (6)	C(3)–S(4)–Ni	107.5 (8)
Ni–S(4)	2.159 (8)	O(4)–C(1)	1.13 (3)	Cl(3)–Sn–Cl(4)	102.3 (3)	Sn–O(1)–C(3)	112 (1)
S(1)–S(3)	3.08 (1)	C(1)–C(4)	1.61 (3)	Cl(3)–Sn–O(1)	89.8 (4)	Sn–O(2)–C(2)	110 (1)
S(1)–S(4)	3.00 (1)	C(2)–C(3)	1.48 (3)	Cl(3)–Sn–O(2)	166.6 (5)	S(1)–C(1)–O(4)	129 (2)
S(1)–C(1)	1.78 (2)			Cl(4)–Sn–O(1)	168.0 (4)	S(2)–C(2)–O(2)	122 (2)
S(2)–S(3)	3.02 (1)			Cl(4)–Sn–O(2)	91.1 (5)	S(4)–C(3)–O(1)	125 (2)
						S(3)–C(4)–O(3)	124 (2)

[a] Bond distances and angles in the $BzPh_3P^+$ cation may be found in Table VII which has been deposited (ref 21).

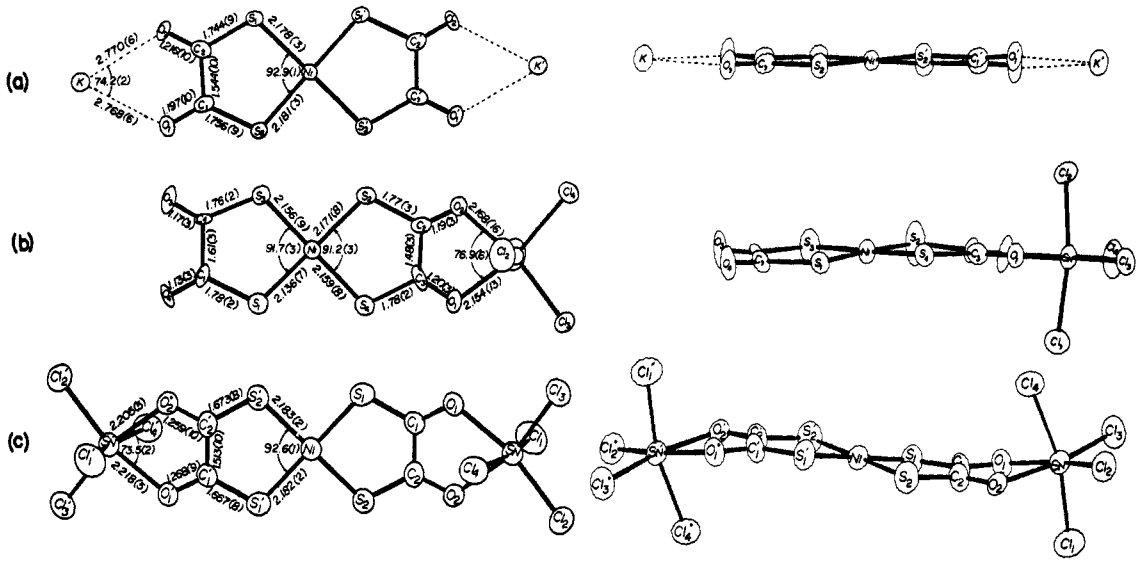

Figure 2. The structures of (a) $Ni(S_2C_2O_2)_2^{2-}$, (b) $[Ni(S_2C_2O_2)_2SnCl_4]^{2-}$, and (c) $[Ni(S_2C_2O_2)_2(SnCl_4)_2]^{2-}$. Thermal vibrational ellipsoids are scaled to enclose 50% probability with the exception of (b) where thermal vibrational ellipsoids are scaled to enclose 20% probability.

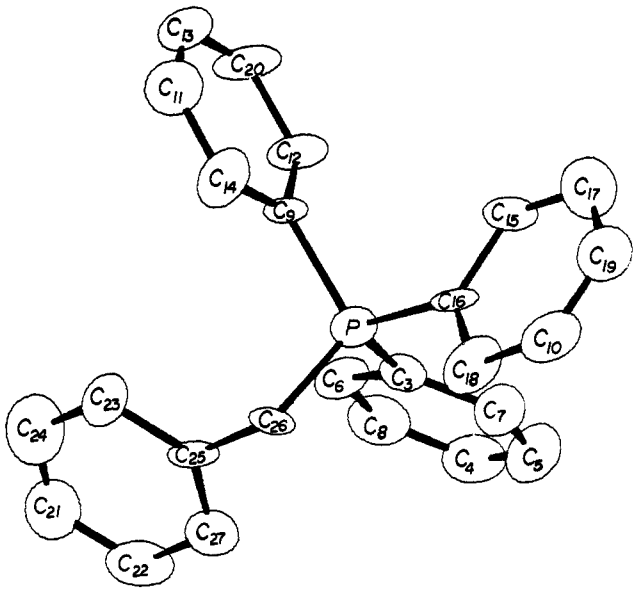

Figure 3. The structure of the $C_7H_7(C_6H_5)_3P^+$ cation in $Ni(Dto)_2(SnCl_4)_2(BzPh_3P)_2$. Vibrational ellipsoids enclose 50% probability.

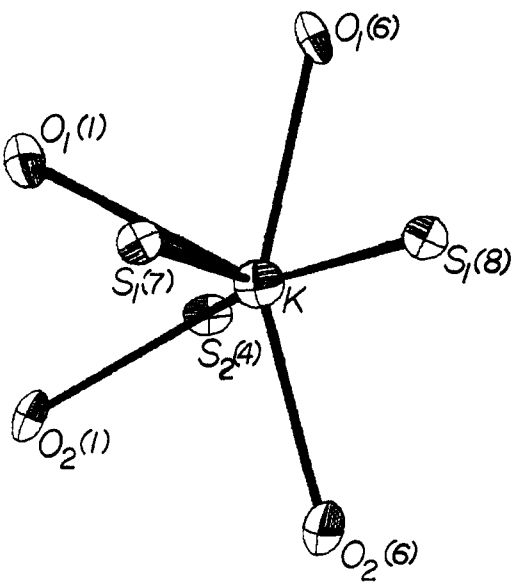

Figure 4. The structure of the KS_3O_4 polyhedron. Vibrational ellipsoids enclose 50% probability. The numbering scheme is identical with the one used in Table IX.

Table VIII. Infrared Spectra of Dithiooxalate Complexes and Their SnX_4 Adducts[a]

$Ni(Dto)_2^{2-}$	$[Ni(Dto)_2\text{-}SnF_4]^{2-}$	$[Ni(Dto)_2\text{-}SnCl_4]^{2-}$	$[Ni(Dto)_2\text{-}(SnCl_4)_2]^{2-}$	$[Ni(Dto)_2\text{-}(SnBr_4)_2]^{2-}$	$[Ni(Dto)_2\text{-}(SnI_4)_2]^{2-}$	$Pd(Dto)_2^{2-}$	$[Pd(Dto)_2\text{-}SnCl_4]^{2-}$	$[Pd(Dto)_2\text{-}(SnCl_4)_2]^{2-}$	$[Pd(Dto)_2\text{-}(SnBr_4)_2]^{2-}$	$[Pd(Dto)_2\text{-}(SnI_4)_2]^{2-}$	Assignment
1605 (s)	1640 (s)	1640 (s)	1470 (s)	1460 (s)	1470 (s)	1618 (s)	1635 (s)	1465 (s)	1460 (s)	1455 (s)	A_1, B_2 (λ_1, λ_7)[b]
1588 (s)	1625 (s)	1613 (s)				1590 (s)	1612 (s)				C=O str
	1460 (s)	1445 (s)					1448 (s)				
1050 (s)	1050 (m)	1052 (m)	1145 (m)	1143 (m)	1140 (m)	1048 (m)	1050 (m)	1150 (s)	1143 (m)	1144 (m)	A_1 (λ_2)[b] ν(C=C)
	1025 (w)	1025 (w)									+ ν(C—S) comb
910 (m)	994 (w)	994 (w)	993 (m)	993 (m)	992 (m)	913 (m)	993 (w)	995 (m)	990 (m)	995 (m)	B_2 (λ_8)[b] δ(C—O)
	900 (w)	898 (w)									+ ν(C—S) comb
614 (mw)	649 (w)	645 (w)	628 (m)	626 (m)	626 (m)	614 (m)	642 (m)	628 (m)	626 (w)	625 (w)	A_1 (λ_3)[b] C—S
	615 (sh)	614 (mw)					628 (m)				str
349 (s)	378 (m)	385 (ms)	378 (s)	375 (s)	375 (s)	317 (s)	261 (m)[c]	*c*	331 (s)	329 (s)	M—S str
	365 (m)	*c*					267 (m)				
	600 (s)	363 (s)	362 (s)	246 (s)	196 (s)		355 (s, br)	355 (s)	248 (s)	194 (s)	Sn—X str modes
	581 (s)	328 (br)	353 (s)	235 (s)	186 (s)		331 (s)	327 (s, br)	234 (s, br)	188 (s)	
	537		333 (s)	227 (sh)	180 (s)		219 (s)	216 (s)	178 (s)	180 (s)	
	327	221 (s)	218 (s)	176 (s)	132 (s)					131 (s)	
	240	184 (s)	173 (s)	131 (s)	105 (s)		168 (s)	169 (s)	131 (s)		Sn—X bending
	212	160 (s)	156 (s)	98 (s)			155 (s)	156 (s)	98 (s)	104 (s)	modes
	282	290 (s)	291 (s)	281 (s)	281 (s)		290 (s)	290 (s)	274 (s)	270 (s)	Sn—O—C def

[a] s = strong, w = weak, br = broad, m = medium, sh = shoulder. Near-infrared spectra taken in Nujol mulls between salt plates. Far-infrared, Nujol mulls between high density polyethylene films. [b] The analogs for a few bands reported in ref 25 for the $Pt(Dto)_2^{2-}$ anion could not be located in the present study because of overlying $BzPh_3P^+$ absorptions. [c] The region of the spectrum where the expected M–S vibration should be observed is obscured by Sn–Cl vibrations.

Table IX. Weighted Least-Squares Planes. Deviations from the Planes (Å) of Atoms Used to Define the Planes

	$K_2Ni(Dto)_2$			$(BzPh_3P)_2Ni(Dto)_2SnCl_4$ Anion				$(BzPh_3P)_2Ni(Dto)_2(SnCl_4)_2$ Anion		
Atom	Plane 1	Plane 2	Plane 3	Atom	Plane 1	Plane 2	Plane 3	Plane 4	Atom	Plane 1	Plane 2	Plane 3
Ni	0.000 (1)			Sn				0.001 (2)	Sn			−0.006 (1)
K			0.000 (2)	Ni	0.003 (4)				Ni	0.000 (3)		
S(1)	0.000 (2)	−0.004 (2)		Cl(3)				−0.005 (8)	Cl(2)			0.013 (3)
S(2)	0.000 (2)	0.003 (2)		Cl(4)				−0.005 (9)	Cl(3)			0.031 (3)
C(1)		−0.004 (8)		S(1)	−0.028 (7)		0.007 (7)		S(1)	0.000 (3)	−0.016 (3)	
C(2)		0.018 (8)		S(2)	−0.052 (10)	0.031 (10)			S(2)	0.000 (3)	0.017 (3)	
O(1)		−0.038 (7)	0.000 (7)	S(3)	0.0314 (9)		0.003 (9)		O(1)		0.076 (6)	0.033 (6)
O(2)		0.028 (6)	0.000 (6)	S(4)	0.0217 (7)	−0.017 (7)			O(2)		−0.080 (6)	0.137 (6)
				O(1)		0.081 (16)		−0.010 (16)	C(1)		0.027 (10)	
				O(2)		−0.130 (20)		−0.031 (20)	C(2)		−0.007 (10)	
				O(3)			0.002 (20)					
				O(4)			0.021 (19)					
				C(1)			−0.034 (22)					
				C(2)		−0.013 (28)						
				C(3)		0.027 (24)						
				C(4)			−0.015 (21)					

Dihedral Angles (deg)

Plane 1–plane 2	1.6	Plane 1–plane 2	6.3	Plane 2–plane 3	5.4	Plane 1–plane 2	9.0
Plane 1–plane 3	2.4	Plane 1–plane 3	1.9	Plane 2–plane 4	4.1	Plane 1–plane 3	26.5
Plane 2–plane 3	1.4	Plane 1–plane 4	9.0	Plane 3–plane 8	8.4	Plane 2–plane 3	17.7

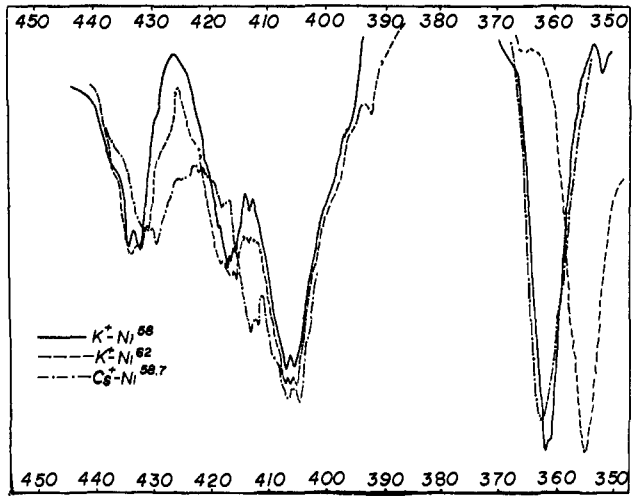

Figure 5. Infrared spectra of isotopically substituted $K_2Ni(S_2C_2O_2)_2$ complexes.

1:1 adducts, which is attributed to the unperturbed ligand, is appreciably different from that of the same vibration in the spectrum of the "parent" $Ni(Dto)_2^{2-}$ complex (1605 cm^{-1}).

A medium intensity band which occurs at 614 cm^{-1} in the spectra of the parent complexes is found at 628 cm^{-1} in the spectra of the 2:1 adducts. Two bands are found in the spectra of the 1:1 adducts at 614 and 645 cm^{-1}, respectively. We assign the 614-cm^{-1} band in the spectra of the parent complexes to a C–S stretching vibration. This vibration undergoes a hypsochromic shift in the adducts which is consistent with the increase in the C–S order.

In the far-ir spectra of both the nickel and palladium "parent" complexes, two bands found at 432 and 417 cm^{-1}, were previously assigned[25] to the M–S stretching vibrations. Similarly two strong bands at 350 and 317 cm^{-1} in the spectra of the nickel and palladium complexes, respectively, were attributed to the C–O deformation mode. Isotopic substitution of ^{58}Ni and ^{62}Ni in the K^+ salt of the parent nickel complex clearly shows that *only the band at 350 cm^{-1} is affected* (Figure 5) and a frequency difference of 7 ± 1 cm^{-1} is observed for the two isotopes. When the potassium cation is replaced by cesium, the bands at 432 and 417 cm^{-1} are shifted to 429 and 413 cm^{-1}, respectively. The above evidence strongly suggests that the assignments made previously are in error and that the vibrations attributed to the C–O deformation mode are instead due to the M–S stretching vibrations.

The stannic halide adducts of the $Ni(Dto)_2^{2-}$ complex show a strong band at 380 cm^{-1}. This band, which is absent from the spectra of the corresponding X-ray isomorphous palladium complexes, is assigned to the Ni–S stretching vibration. A band present in all of the $Pd(Dto)_2^{2-}$ adducts at 330 cm^{-1} but absent from the spectra of the $Ni(Dto)_2^{2-}$ adducts is similarly assigned to the Pd–S stretching vibration.

The lower frequencies of the M–S stretching vibrations[26] in the spectra of the $(BzPh_3P)_2Ni(Dto)_2$ and $(BzPh_3P)_2Pd(Dto)_2$ complexes, found at 350 and 317 cm^{-1}, respectively, suggest that *addition of stannic halide brings about a strengthening of the M–S bond.*

(26) The observed differences in the frequencies of the M–S stretching vibrations could be larger than the ones actually observed since kinematic effects would tend to lower the frequency of the M–S stretch in the $SnCl_4$ adducts.

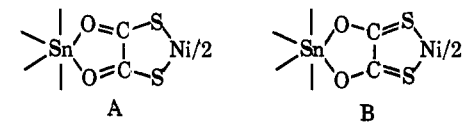

Figure 6. Two of the important resonance forms describing the $[Ni(S_2C_2O_2)_2(SnX_4)_2]^{2-}$ complexes.

For compounds of the type ML_2X_4 (C_{2v} symmetry) group theory predicts four M–X stretching modes ($2A_1 + B_1 + B_2$). Beattie and Rule,[27] by transferring force constant data from $SnCl_6^{2-}$ directly to the $SnCl_4$ residue in a cis adduct, calculated the approximate positions of these bands as a_1, 243 and 310 cm^{-1}; b_1, 332; b_2, 297. Similar patterns of bands are found in the spectra of the stannic halide adducts of the $M(Dto)_2^{2-}$ complexes. Calculations of the ν(Sn-I)/ν(Sn-Cl), ν(Sn-I)/ν(Sn-Br), and ν(Sn-Br)/ν(Sn-Cl) ratios for all of these bands give values of roughly 0.6, 0.8, and 0.7 which agree well with similar values quoted in the literature.[28-30]

Bands occurring below 250 cm^{-1} in the $SnCl_4$ adducts, 200 cm^{-1} in the $SnBr_4$ adducts, and 150 cm^{-1} in the SnI_4 adducts are assigned to X–Sn–X bending modes. The Sn–F stretching vibrations in the $[Ni(Dto)_2SnF_4]^{2-}$ complex found at 600, 581, 537, and 327 cm^{-1} are in agreement with similar values reported in the literature.[31]

Solid-State Structure Determinations. The coordination geometry about the nickel atom in each one of the structures is four coordinate and planar. The bond length data (Tables III, V, VII) for the C–S, C–O, and C–C bonds show that the ligands in the "parent" complex are significantly different than the bridging ones in the adducts. These differences reflect the changes indicated by the infrared data and strongly suggest that in the adducts resonance form B (Figure 6) contributes to the overall description of the structure considerably more than a similar resonance form does in the structure of the $Ni(Dto)_2^{2-}$ complex. The stannic chloride adducts exhibit the "stepped"[32] type of structure where the MS_4, $S_2C_2O_2$, and O_2SnCl_2 molecular fragments are individually planar but not coplanar. In the $K_2Ni(Dto)_2$ complex the KO_2 and $S_2C_2O_2$ moieties are nearly coplanar; however, the NiS_4 rhombus is distorted from planarity due to a twisting of the ligands by 9° relative to each other (Figure 2). The nickel atoms are located on the twofold axes. Appropriate best planes and dihedral angles are shown in Table IX.

Although charge is delocalized away from the sulfur atoms upon adduct formation, the lengths of the Ni–S bonds in the 2:1 adduct are very similar to those found in the $K_2Ni(Dto)_2$ complex. The strengthening in the Ni–S bond in the SnX_4 adducts, implied by the infrared

(27) I. R. Beattie and L. Rule, *J. Chem. Soc.*, 3267 (1964).
(28) F. A. Cotton, R. M. Wing, and R. A. Zimmerman, *Inorg. Chem.*, **6**, 11 (1967).
(29) R. J. H. Clark, *Rec. Chem. Progr.*, **26**, 269 (1965).
(30) K. Nakamoto, "Infrared Spectra of Inorganic and Coordination Compounds," Wiley, New York, N. Y., 1970, p 214.
(31) C. J. Wilkins and H. M. Haendler, *J. Chem. Soc.*, 3174 (1965).
(32) R. H. Holm and M. J. O'Connor, *Progr. Inorg. Chem.*, **14**, 241 (1972).

data, is not apparent from this structure.[33] All four of the symmetry-independent Ni–S bonds in the 1:1 adduct are shorter than those found in the other two structures. The Ni–S bonds to the nonbridging ligand in this complex are significantly (3.5σ) shorter than those found in the structure of the parent complex. These data combined with the infrared results suggest that the addition of one $SnCl_4$ molecule to the $Ni(Dto)_2^{2-}$ complex affects the bonding of the nonbridging ligand at the opposite end of the complex anion (*vide infra*). A comparison of the O_1–Sn–O_2 angle and the Sn–O bond lengths in the 1:1 adduct to corresponding values in the 2:1 adduct (Figure 2) indicates slightly stronger Sn–O interactions in the former.

The interligand and intraligand bond lengths and bond angles in the coordination spheres of the nickel atoms are comparable to those found in the structures of other planar 1,2-dithiolato complexes of Ni(II)[34,35] and will not be discussed any further. The tin is octahedrally coordinated, in both of the $SnCl_4$ adducts (Figure 2), the oxygen atoms being in the cis configuration. The octahedra are somewhat distorted with a Cl_{ax}–Sn–Cl_{ax} angle of 165.6 (1) and 170.0 (3)° for the 2:1 and 1:1 adducts, respectively. The Sn–Cl bond lengths, Sn–Cl_{ax} = 2.395 (3), Sn–Cl_{eq} = 2.347 (2) and Sn–Cl_{ax} = 2.380 (8), Sn–Cl_{eq} = 2.338 (7) Å, in the two structures, indicate significant difference between axial and equatorial chlorine atoms and are similar to those reported[36-41] in structural determinations of other cis-octahedral SnX_4L_2 complexes. The reader is referred to these papers for a discussion of the electronic and steric effects which are believed to influence the structures of these compounds.

The bond distances and angles in the three $(C_7H_7)(C_6H_5)_3P^+$ cations are close to normal values. Bond lengths and bond angles[42] for one of these cations (Figure 3) are found in Table V.

The coordination geometry of the seven-coordinate potassium ion (Figure 4) in $K_2Ni(Dto)_2$ is described as an irregular polyhedron defined by four oxygen and three sulfur atoms. Bond lengths and bond angles in this polyhedron are shown in Table X.

Electronic Structures. Coordination of a stannic halide molecule to the α-diketone portion of the S-coordinated dithiooxalate ligand is expected to decrease the S → M σ bonding and consequently weaken the M–S bond. However, M–S π back-bonding is expected to show an opposing effect, *i.e.*, strengthening of the M–S bond. The data at hand suggest that the latter effect is prevalent causing an apparently stronger M–S bond in the adduct. The above conclusion is further reinforced by a recent analysis of the epr spectra of the bisdithiooxalate iron nitrosyl complex anion, $[Fe(Dto)_2NO]^{2-}$, and its stannic chloride adduct, $[(SnCl_4)_2Fe(Dto)_2NO]^{2-}$.[43] The percentage of nitrogen 2s and 2p character of the half-filled MO in the unperturbed complex was calculated as 2.63 and 2.72%, respectively. On addition of $SnCl_4$ the s character changes to 2.28% and the p character becomes 3.36%. The increase in the Fe–NO π bonding in the adducts apparently occurs as a result of enhanced "mixing" of the π* (NO) orbitals with the metal d_{xz} and d_{yz} orbitals.[43] The structural data on the 1:1 adduct show four Ni–S bonds which are not significantly different from each other and are slightly shorter than those in the "parent" complex and the 2:1 adduct. These data can be explained if one realizes that whereas π back-bonding accounts for the strengthening of the M–S bond with the bridging ligand, enhanced σ bonding accounts for equally strong Ni–S bonds with the nonbridging ligand. An increase in L → Ni σ bonding is expected to occur with the nonbridging ligand as Ni → L π back-bonding to the bridging ligand increases the positive charge on the metal ion. These arguments are further reenforced by the difference in the C–O stretching frequencies observed for the nonbridging ligands in the 1:1 adduct and the parent complex at 1640 and 1605 cm^{-1}, respectively.[44,45]

Table X. Selected Structural Details[a] of the KO_4S_8 Coordination Polyhedron

Bond lengths,[b] Å		Bond angles, deg	
K–O_1(1)	2.768 (10)	O_1(1)–K–O_2(1)	58.2 (3)
–O_2(1)	2.770 (10)	O_2(1)–K–O_2(6)	131.3 (4)
–O_1(6)	2.685 (7)	O_2(6)–K–O_1(6)	150.0 (3)
–O_2(6)	2.688 (7)	O_1(6)–K–O_1(1)	132.2 (3)
		S_1(7)–K–S_2(4)	149.6 (2)
–S_1(7)	3.431 (5)	S_2(4)–K–S_1(8)	158.7 (3)
–S_1(8)	3.456 (5)	S_1(8)–K–S_1(7)	51.5 (3)
–S_2(4)	3.400 (5)	S_1(7)–K–S_2(4)	168.8 (2)
		O_1(6)–K–S_1(8)	119.4 (2)
–S_2(6)	3.980 (4)	O_1(6)–K–S_1(7)	96.4 (3)
–O_1(4)	3.876 (10)	O_1(6)–K–S_2(4)	87.8 (3)
		O_2(6)–K–S_1(8)	93.9 (3)
		O_2(6)–K–S_1(7)	105.9 (3)
		O_2(6)–K–S_2(4)	83.0 (3)

[a] The numbers in parentheses following the atomic designations refer to the eight symmetry transformations in the space group C_2/c: (1) x, y, z; (2) $\bar{x}, y, \bar{z}$; (3) $\bar{x}, \bar{y}, \bar{z}$; (4) $x, \bar{y}, z$; (5) $\frac{1}{2} + x, \frac{1}{2} + y, z$; (6) $\frac{1}{2} - x, \frac{1}{2} + y, \frac{1}{2} - z$; (7) $\frac{1}{2} - x, \frac{1}{2} - y, -z$; (8) $\frac{1}{2} + x, \frac{1}{2} - y, \frac{1}{2} + z$. [b] Confined to neighboring atoms within a 4 Å sphere around the potassium ion.

(33) The accuracy in the measurement of the infrared vibrational frequency of a bond (±1 cm^{-1}) allows the detection of relatively small changes in the force constant. The same changes have such a small effect on the bond lengths that they cannot be detected within the accuracy limits of the crystallographic measurements.

(34) R. Eisenberg and J. A. Ibers, *Inorg. Chem.*, 4, 605 (1965).

(35) R. Eisenberg, J. A. Ibers, R. J. H. Clark, and H. B. Gray, *J. Amer. Chem. Soc.*, 86, 113 (1964).

(36) Y. Hermodsson, *Acta Crystallogr.*, 13, 656 (1960).

(37) I. Lindqvist, "Inorganic Adduct Molecules of Oxo-Compounds," Springer-Verlag, Berlin, 1963, p 73.

(38) C. I. Branden, *Acta Chem. Scand.*, 17, 759 (1963).

(39) D. M. Barnhart, C. N. Caughlan, and M. Ul-Haque, *Inorg. Chem.*, 7, 1135 (1968).

(40) M. Webster and H. E. Blayden, *J. Chem. Soc. A*, 2443 (1969).

(41) A. D. Adley, P. H. Bird, A. R. Fraser, and M. Onyszchuk, *Inorg. Chem.*, 11, 1402 (1972).

(42) Bond angles and bond lengths for the two $(C_7H_7)(C_6H_5)_3P^+$ cations which accompany the $[Ni(Dto)_2SnCl_4]^{2-}$ complex and figures illustrating the numbering scheme have been deposited (see ref 21).

(43) W. V. Sweeney and R. E. Coffman, *J. Phys. Chem.*, 76, 49 (1972).

(44) The failure to obtain the 2:1 adducts with SnF_4 and the 1:1 adducts with either $SnBr_4$ or SnI_4 qualitatively indicates that the donor properties of the nonbridging ligand in the 1:1 adducts vary as dictated by the acid strength of the SnX_4 molecule.

(45) Similar effects have been observed in other studies of ternary interactions of Lewis acids with metal complexes of bifunctional ligands. Thus addition of Hg^{2+} to the $(H_2O)_5CrNCS^{2+}$ complex resulted in an adduct, $(H_2O)_5CrNCSHg^{4+}$, in which the hypsochromic shifts of the d–d and L → M charge transfer absorptions were attributed to Hg^{2+} induced M–NCS π back-bonding.[46] Similarly in the structure of $(CH_3CN)_4Mo(CN)_4$[47] (obtained by CH_3^+ addition to $Mo(CN)_8^{4-}$) the better π-acceptor isocyanide ligands are positioned to accept electron density from the filled $d_{x^2-y^2}$ orbital of the molybdenum atom. In this complex shorter Mo–C bond lengths were found for the isocyanide ligands as well as a ligand field stronger than that found in $Mo(CN)_8^{4-}$.

(46) J. N. Armor and A. Haim, *J. Amer. Chem. Soc.*, 93, 867 (1971).

(47) M. Novotny, D. F. Lewis, and S. J. Lippard, *J. Amer. Chem. Soc.*, 94, 6961 (1972).

Table XI. Electronic Spectra of the Metal–Dithiooxalato Complexes and Their Stannic Halide Adducts in Dichloromethane Solution[a]

	Absorption maxima, $cm^{-1} \times 10^3$				
$Ni(Dto)_2^{2-}$ [b]	17.8 (2.3) sh[c]	19.9 (3.5)	32.7 (18.5)		
$[Ni(Dto)_2SnCl_4]^{2-}$	15.2 (3.2)	15.9 (3.2)	18.2 sh[c]	33.2 sh	
$[Ni(Dto)_2(SnCl_4)_2]^{2-}$	16.0 (6.9)	17.2 (4.9)	18.5 (3.3)	32.5 (49.0)	
$[Ni(Dto)_2(SnBr_4)_2]^{2-}$	16.0 (6.2)	17.2 (4.2)	18.6 (2.8)	27.8 (16.5)	32.3 (37.0)
$[Ni(Dto)_2(SnI_4)_2]^{2-}$	15.9 (5.3)	18.5 (2.8)	27.9 (17.5)	33.0 (41.5)	
$Pd(Dto)_2^{2-}$	25.1 (7.2)	36.4 (42.0)	41.3 (17.0)		
$[Pd(Dto)_2(SnCl_4)]^{2-}$	22.5 (5.3)	23.5 (5.2)	27.0 (3.6)		
$[Pd(Dto)_2(SnCl_4)_2]^{2-}$	22.2 (7.8) sh	24.1 (12.8)	27.4 (8.2) sh		
$[Pd(Dto)_2(SnBr_4)_2]^{2-}$	22.2 (8.6) sh	23.8 (13.2)	26.2 (9.1) sh	27.6 (8.1)	
$[Pd(Dto)_2(SnI_4)_2]^{2-}$	22.0 (2.7)	27.6 (5.1)			

[a] Molar extinction coefficients are given in parentheses ($\epsilon \times 10^{-3}$). [b] Data reported in ref 1. [c] d–d band.

Table XII. Cyclic Voltammetry Data for the $[M(Dto)_2(SnX_4)_2]^{2-}$ Complexes in Dichloromethane Solution[a]

Complex	$E_{1/2}$,[b] V	i_p/e,[c] μA/m*M*	Rev (r) or irrev (i)
$[Ni(Dto)_2SnF_4]^{2-}$	−0.99	+40	r
$[Ni(Dto)_2SnCl_4]^{2-}$	−0.94	+38	r
$[Pd(Dto)_2SnCl_4]^{2-}$	−0.91	+39	r
$[Ni(Dto)_2(SnCl_4)_2]^{2-}$	−0.51	+36	r
	−0.93	+38	r
$[Pd(Dto)_2(SnCl_4)_2]^{2-}$	−0.56	+35	r
	−0.90	+38	r
$[Ni(Dto)_2(SnBr_4)_2]^{2-}$	−0.55[d]		i
$[Pd(Dto)_2(SnBr_4)_2]^{2-}$	−0.63[d]		i
$[Ni(Dto)_2(SnI_4)_2]^{2-}$	−0.42		i
$[Pd(Dto)_2(SnI_4)_2]^{2-}$[e]	−0.37		i
$[Ni(MNT)_2]^{2-}$ [d]	+0.18	−40	r
$[Ni(MNT)_2]^{-}$ [d]	−0.18	+46	r

[a] Using 0.2 *M* tetra-*n*-butylammonium perchlorate as supporting electrolyte and a stationary platinum sphere electrode. [b] *Vs.* Ag/AgI reference electrode. [c] Measurements of potentials and i_p (peak currents) at a voltage scan speed of 0.5 V/sec. Positive current indicates reduction and negative current oxidation. [d] The current densities observed for the known one-electron oxidation and reduction of $Ni(MNT)_2^{2-}$ and $Ni(MNT)_2^{-}$, respectively, are similar to those of the SnX_4–$M(Dto)_2^{2-}$ adducts and suggest that the latter also undergo one-electron transfer. [e] The "parent" nickel(II) and palladium(II) dithiooxalato complexes do not undergo reversible redox reactions; furthermore the anhydrous stannic halides in dichloromethane undergo ill-defined irreversible reduction.

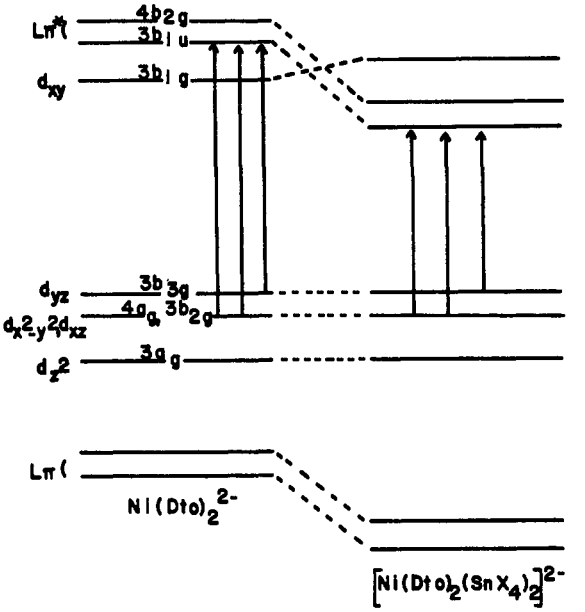

Figure 7. Energy level diagram for $M(Dto)_2^{2-}$ and $[M(Dto)_2(SnCl_4)_n]^{2-}$ complexes.

Shriver and coworkers calculated[48] the orbital energies of $CN^- + H^+$ as a function of the N–H distance and observed a decrease of the σ, σ*, π, and π* orbital energies as the N–H distance decreased. Assuming that addition of stannic halide affects the dithiooxalate ligand orbitals in a similar fashion, the changes in bonding previously described can be explained. The lowering of the ligand π and π* energies in the adducts also is consistent with the low energy of the first high-intensity charge transfer band in the spectra of the adducts (Figure 7, Table XI). This band, which occurs at higher energies in the spectra of the $M(Dto)_2^{2-}$ complexes, was assigned[49] to a M → L ($b_{3g} \rightarrow L(\pi^*)$) charge transfer absorption.

As the energy difference $E\pi^*(L) - E_{d_{xz},d_{yz}}$ (Figure 7) becomes smaller[50] the π*(L) character of the symmetry-compatible d_{xz} and d_{yz} orbitals increases and so does the M–L π bonding. The decrease in the energy separation of the L(π*) and d_{xz} and d_{yz} orbitals is aptly illustrated in the bathochromic shift of the M → L charge transfer band.

Electrochemistry. The data in Table XII describe the electrochemical behavior of the stannic halide adducts.

Well-defined reversible reduction waves were observed only for the $SnCl_4$ and SnF_4 adducts, whereas only quasireversible or irreversible reductions were observed with the $SnBr_4$ and SnI_4 adducts, respectively. An interesting feature of the reduction properties of the complexes is that the 1:1 adducts with $SnCl_4$ or SnF_4 undergo a one-electron reversible reduction while the 2:1 adducts with $SnCl_4$ undergo reversible reduction in two one-electron steps. Although the stannic halide adducts can formally be classified with the anionic dithiolene complexes, they do not undergo the reversible oxidations characteristic of the anionic dithiolenes.[13,51] On the contrary they reversibly gain electrons. The redox properties of the adducts could be explained as ligand centered reductions by formally describing these complexes either as Sn(IV) ortho

(48) (a) D. F. Shriver, S. A. Shriver, and S. E. Anderson, *Inorg. Chem.*, 4, 725 (1965); (b) J. J. Rupp and D. F. Shriver, *ibid.*, 6, 755 (1967), and references therein.

(49) A. R. Latham, V. C. Hascall, and H. B. Gray, *Inorg. Chem.*, 4, 788 (1965).

(50) The energy of the $4a_g$ orbital was placed higher than that of the $3b_{3g}$ orbital to account for the intensities of the M–L charge transfer bands. We suggest that electronically the planar, anionic dithiooxalate complexes are best described in terms of a $^1B_{3g}$ ground state which would result if the $4a_g$ and $3b_{3g}$ orbitals are interchanged. This description is in accord with the generally accepted ground state in the planar anionic dithioleneś[1] and consistent with the electronic properties of the stannic halide adducts of the dithiooxalate complexes.

(51) J. A. McCleverty, *Progr. Inorg. Chem.*, 10, 49 (1968).

quinone complexes (Figure 6A) or as oxidized dithiolene complexes (Figure 6B).

Perhaps a better interpretation of the reduction properties, however, is one that places the added electrons in a ligand π^* MO of b_{1u} symmetry (Figure 7). The bathochromic shift of the M → L ($b_{3g} \rightarrow L\pi^*$) transition in the electronic spectra of the adducts and the energy of this transition relative to that of the d–d transition[52] suggest that, in the adducts, the ligand π^* MO of b_{1u} symmetry is of lower energy than the d_{xy} metal orbital. The per cent metal character of the b_{1u} MO cannot be ascertained, although the reduction properties of the adducts and the stability of the reduction products clearly depend[55] on the type of metal atom bonded to the α-diketone portion of the coordinated dithiooxalate ligand and to a lesser extent on the environment about this atom.

Acknowledgments. The authors wish to thank Mr. D. Piltingsrud for assistance with some of the infrared measurements, the Donors of the Petroleum Research Fund, administered by the American Chemical Society, for a grant (PRF No. 1775-G3), the National Science Foundation for a grant (GP 28567), and the Graduate College of the University of Iowa for granting the necessary funds for the purchase of computer time.

(52) From the Δ_0 reported by Carlin and Canziani[53] for $Co(Dto)_3^{3-}$ the energy of the Δ_1 transition for the $Ni(Dto)_2^{2-}$ is calculated to occur at 17,700 cm^{-1}. A shoulder found at 17,700 cm^{-1} in the spectrum of $Ni(Dto)_2^{2-}$ has been assigned[49] to the Δ_1 transition. In agreement with the stronger M–S bonding in the adducts is the fact that, in the adducts, larger values of Δ_0 are generally observed.[54]

(53) R. L. Carlin and F. Canziani, *J. Chem. Phys.*, **40**, 371 (1964).

(54) D. Coucouvanis and D. Piltingsrud, *J. Amer. Chem. Soc.*, in press.

(55) With $TiCl_4$ or $SnCl_2$ the dithiooxalate complexes form adducts which undergo ill-defined irreversible reductions.

Application of Collisional Activation Spectra to the Elucidation of Organic Ion Structures[1,2]

F. W. McLafferty,*[2a] Richard Kornfeld, W. F. Haddon, Karsten Levsen, Ikuo Sakai,[2c] P. F. Bente III, Shih-Chuan Tsai, and H. D. R. Schuddemage

Contribution from the Department of Chemistry, Cornell University, Ithaca, New York 14850. *Received September 5, 1972*

Abstract: The relative abundances of most product ions resulting from collisional decomposition of a gaseous ion are shown to depend only on the ion's structure, and not on its internal energy. The structure of an ion can be characterized by matching its collisional activation (CA) spectrum with that of a known reference ion; $C_2H_5O^+$, $C_3H_6O^+$, $C_7H_8^+$, and $C_{13}H_9^+$ ions are used as examples. The resemblance of ion decomposition pathways of CA spectra to those of conventional mass spectra makes possible the interpretation of CA spectra to provide structural information of unknown ions.

The structure characterization of gaseous positive ions has been the subject of an increasing number of studies involving ion–molecule[3] and unimolecular–ion reactions.[4,5] Definitive structural information is often difficult to obtain; reactivity behavior studies can be subject to unpredictable effects of ion internal energy and usually require isotopic labeling, and thermochemical energy requirements must be interpreted with caution. The importance of ion structures for both fundamental studies of ion reactions and determination of unknown molecular structures would make valuable a simple, direct method for ion structure identification and characterization. This paper describes the use of collisional activation (CA) spectra[6] in such applications.

Increasing the pressure in a field-free drift region of a mass spectrometer causes ion–neutral collisions in which some of the ion's kinetic energy is converted into internal energy. The resulting ion decomposition products (the "CA spectrum")[6] can be studied using the same techniques developed for unimolecular metastable ion decompositions.[4b,7] CA spectra, like metastable ion (MI) spectra,[4b] appear to add on "extra dimension" of information to a normal electron-impact (EI) mass spectrum in that a CA spectrum can be obtained for each product ion of an EI spectrum,

(1) Metastable Ion Characteristics. XXIV. Part XXIII: D. J. McAdoo, P. F. Bente III, F. W. McLafferty, M. L. Gross, and C. Lifshitz, *Org. Mass Spectrom.*, in press.

(2) (a) John Simon Guggenheim Memorial Foundation Fellow, 1972; (b) taken in part from the Cornell University Ph.D. Theses of R. K., 1971, and S.-C. T., 1972; (c) visiting scientist on leave from Toray Industries, Kamakura, Japan. (d) We are grateful to the National Institutes of Health (GM 16609) and the Army Research Office (D-31-124-G1117) for generous support of this work.

(3) (a) J. L. Beauchamp, *Annu. Rev. Phys. Chem.*, **22**, 527 (1971); (b) G. Eadon, J. Diekman, and C. Djerassi, *J. Amer. Chem. Soc.*, **92**, 6205 (1970); (c) J. L. Beauchamp and R. C. Dunbar, *ibid.*, **92**, 1477 (1970); (d) D. J, McAdoo, P. F. Bente III, and F. W. McLafferty, *ibid.*, **94**, 2027 (1972).

(4) (a) H. Budzikiewicz, C. Djerassi, and D. H. Williams, "Mass Spectrometry of Organic Compounds," Holden-Day, San Francisco, Calif., 1967; (b) K. R. Jennings in "Mass Spectrometry; Techniques and Applications," G. W. A. Milne, Ed., Wiley-Interscience, New York, N. Y., 1971, p 419; (c) A. G. Harrison and C. W. Tsang in "Biochemical Applications of Mass Spectrometry," G. R. Waller, Ed., Wiley-Interscience, New York, N. Y., 1972, p 135.

(5) (a) L. Friedman, F. A. Long, and M. Wolfsberg, *J. Chem. Phys.*, 27, 613 (1957); (b) T. W. Shannon and F. W. McLafferty, *J. Amer. Chem. Soc.*, **88**, 5021 (1966); (c) K. M. A. Refaey and W. A. Chupka, *J. Chem. Phys.*, **48**, 5205 (1968); (d) A. G. Harrison and B. G. Keyes, *J. Amer. Chem. Soc.*, 90, 5046 (1968).

(6) (a) W. F. Haddon and F. W. McLafferty, *J. Amer. Chem. Soc.*, **90**, 4745 (1968); (b) F. W. McLafferty and H. D. R. Schuddemage, *ibid.*, **91**, 1866 (1969); (c) F. W. McLafferty, P. F. Bente III, R. Kornfeld, S.-C. Tsai, and I. Howe, *ibid.*, **95**, 2120 (1973).

(7) T. Wachs, P. F. Bente III, and F. W. McLafferty, *Int. J. Mass Spectrom. Ion Phys.*, **9**, 333 (1972).